



Supporting Information

The Energetics of a Three-State Protein Folding System Probed by High-Pressure Relaxation Dispersion NMR Spectroscopy

Vitali Tugarinov, David S. Libich, Virginia Meyer, Julien Roche, and G. Marius Clore**

anie_201505416_sm_miscellaneous_information.pdf

Supporting Information

NMR Sample Preparation. The plasmid encoding the triple mutant (A39V/N53P/V55L; hereafter referred to as Fyn SH3-VPL) of the *Gallus gallus* Fyn SH3 domain (T85-D142) was constructed as described previously,^{1,2} codon optimized and synthesized by Genscript (Piscataway, NJ). The plasmid has an N-terminal His₆-Tag and a TEV (tobacco etch virus protease³) cleavage site positioned such that the final protein product retains the sequence GAMVQIS at the N-terminus and a C-terminal Arg residue. The resulting construct was cloned into the pET21a expression vector and expressed in BL21 Star (DE3) *E.Coli* cells (Life Technologies NY) using minimal medium with ¹⁵NH₄Cl as the sole nitrogen source. Purification was carried out as described previously.⁴ The [U-¹⁵N]-labeled sample of VPL-FynSH3 (1 mM in protein concentration) was dissolved in 50 mM sodium phosphate buffer, pH 7.0, 0.2 mM EDTA, 0.05% w/v NaN₃ and 10% v/v D₂O.

NMR spectroscopy. NMR experiments were recorded at 35 °C using Bruker Avance-III spectrometers operating at ¹H frequencies of 800.1 MHz (equipped with a Bruker TCI z-axis gradient cryogenic probe) and 500.1 MHz (equipped with a Bruker triple resonance x,y,z-gradient room temperature probe). Temperature differences between spectrometers were corrected by matching the chemical shift difference between residual water and 4,4-dimethyl-4-silapentane-1-sulfonic acid (DSS, 0 ppm) in a sample containing 50 mM sodium phosphate, pH 7.0, 0.2 mM EDTA, 0.5% w/v DSS, 0.05% NaN₃ and 99.9% D₂O. A commercial ceramic high-pressure NMR cell and an automatic pump system (Daedalus Innovations, Philadelphia, PA) were used to vary the pressure from 1 to 2500 bar.

¹⁵N relaxation dispersion experiments were acquired using a ¹⁵N-Carr-Purcell-Meiboom-Gill (CPMG)⁵ scheme with amide proton decoupling (¹H_N-CW ¹⁵N-CPMG)⁶ at 500 and 800 MHz spectrometer fields and six pressures: 1, 500, 1000, 1500, 2000, and 2500 bar. ¹⁵N relaxation dispersion with a constant ¹⁵N relaxation period of 100 ms were obtained at CPMG field strengths, ν_{CPMG} , of 20, 30, 40, 50, 60, 70, 80, 100, 120, 140, 160, 200, 260, 320, 400, 500, 600, 700, 800, 900 and 1000 Hz, where $\nu_{CPMG} = 1/2\tau_{CP}$, and τ_{CP} is the time between 180° ¹⁵N CPMG pulses. A field strength of 12 kHz was used for ¹H_N-CW decoupling. An experiment recorded with the relaxation period omitted served as a reference for the calculation of effective R_2 rates as a function of ν_{CPMG} field strength. Experiments with $\nu_{CPMG} = 20$ and 800 Hz were repeated at each pressure and used to estimate the standard errors in the measured R_2^{eff} values. Note that the ¹⁵N-CPMG scheme with ¹H_N-CW decoupling effectively measures the relaxation rates of in-phase ¹⁵N coherences and allows the use of an odd number of CPMG cycles during each half of the constant time relaxation period.⁶

Analysis of pressure-dependent relaxation dispersion data. At 35 °C VPL-FynSH3 undergoes three-site exchange between the major folded state **F**, a sparsely-populated folding intermediate **I**, and the unfolded state **U**:^{1,2}



The evolution of magnetization during the CPMG constant time period for this three-state system can be represented by:

$$M(t) = (AA^* A^* A)^n M(0) \quad [\text{Eq. S2}]$$

where $M = [M^{\text{F}}; M^{\text{I}}; M^{\text{U}}]^T$; M^n denotes the transverse magnetization of state n ; T denotes transposition; $A = \exp(-R\tau_{CP}/2)$; A^* is the complex conjugate of A ; n is the number of CPMG cycles used; τ_{CP} is the time interval between two consecutive 180° pulses in the CPMG pulse train; and the effective transverse relaxation rate $R_{2,\text{eff}} = R_2^{\text{cs}} + R_2^{\text{rel}} + R_2^{\text{ex}}$:

$$R_2^{\text{cs}} = i \begin{bmatrix} 0 & 0 & 0 \\ 0 & \Delta\varpi^{\text{F-I}} & 0 \\ 0 & 0 & \Delta\varpi^{\text{F-U}} \end{bmatrix} \quad [\text{Eq. S3}]$$

$$R_2^{\text{rel}} = \begin{bmatrix} R_2^{\text{F}} & 0 & 0 \\ 0 & R_2^{\text{I}} & 0 \\ 0 & 0 & R_2^{\text{U}} \end{bmatrix} \quad [\text{Eq. S4}]$$

$$R_2^{\text{ex}} = \begin{bmatrix} k_{\text{FI}} & -k_{\text{IF}} & 0 \\ -k_{\text{FI}} & k_{\text{IF}} + k_{\text{IU}} & -k_{\text{UI}} \\ 0 & -k_{\text{IU}} & k_{\text{UI}} \end{bmatrix} \quad [\text{Eq. S5}]$$

where $\Delta\varpi^{m-n}$ is the difference between chemical shifts of states n and m , ($\Delta\varpi^n - \Delta\varpi^m$), R_2^n is the transverse relaxation of state n in the absence of exchange, and the rate constants are as defined in Scheme S1.

The data for all VPL-FynSH3 residues exhibiting relaxation dispersion acquired at all six pressures were fit simultaneously by minimizing the sum of squared differences, χ^2 , between the observed

transverse effective relaxation rates, $R_{2,\text{eff}}$, and those calculated for each ν_{CPMG} value using Eqs. [S2]-[S5] with an in-house Matlab program:

$$\chi^2 = \sum_i \sum_j \sum_{k=1}^2 \left(\frac{R_{2,\text{eff}}^{\text{obs}, i,j,k} - R_{2,\text{eff}}^{\text{calc}, i,j,k}}{\sigma_{R_{2,\text{eff}}^{\text{obs}, i,j,k}}} \right)^2 \quad [\text{Eq. S6}]$$

where the subscripts i, j , and k refer to residue number, the pressure value ($j = 1 \div 6$) and ${}^1\text{H}$ spectrometer frequency (500 and 800 MHz), respectively; and σ is the uncertainty in $R_{2,\text{eff}}$ as estimated from duplicate measurements at two ν_{CPMG} frequencies (see ‘NMR Spectroscopy’). The intrinsic R_2 values for all the states were set equal ($R_2^F = R_2^I = R_2^U$). It has previously been shown that for exchanging systems with highly skewed populations ($p_F \gg p_I, p_U$), as is the case in the present study, this obviously oversimplifying assumption introduces little bias in the extracted exchange parameters.⁷ The dependence of the differences between chemical shifts of states n and m , $\Delta\varpi^{m-n}$, on pressure was modeled according to the quadratic relationship:

$$\Delta\varpi^{m-n}(P) = \Delta\varpi_0^{m-n} + \Delta\varpi_1^{m-n}(P - P_0) + \Delta\varpi_2^{m-n}(P - P_0)^2 \quad [\text{Eq. S7}]$$

where $\Delta\varpi_0^{m-n}$ is the difference in chemical shifts between states n and m at 1 bar, and $P_0 = 1$ bar. The space of residue-specific fitted parameters thus includes: $\{R_{2,j}^{500}; R_{2,j}^{800}; \Delta\varpi_0^{\text{F-I}}; \Delta\varpi_0^{\text{F-U}}; \Delta\varpi_1^{\text{F-I}}; \Delta\varpi_1^{\text{F-U}}; \Delta\varpi_2^{\text{F-I}}; \Delta\varpi_2^{\text{F-U}}\}$, where $R_{2,j}^k$ denotes the intrinsic R_2 (in the absence of exchange) at pressure j and spectrometer field k (500 and 800 MHz), and $\Delta\varpi_i^{m-n}$ are variable parameters denoting the changes in chemical shifts between states m and n ($i = 0, 1, 2$). A total of 46 residues in FynSH3-VPL (T2-V58) showing relaxation dispersion at least at one pressure were included in the global fit of the data at 6 pressure values resulting in $46 \times 6 \times 2 + 46 \times 6 = 828$ residue-specific parameters. The residues E5, S52 and A56 were excluded from the fits because of very low signal-to-noise ratios of the corresponding cross-peaks in the ${}^1\text{H}-{}^{15}\text{N}$ correlation spectra.

The dependence of each of the four rate constants in Scheme [S1] on pressure was modeled using either a linear relationship (model 1),

$$k_{nm}(P) = k_{nm}^0 \exp\{-\Delta V_{\text{TS}_{mn}-n}(P - P_0) / RT\} \quad [\text{Eq. S8}]$$

Or a quadratic relationship (model 2) incorporating isothermal compressibility,

$$k_{nm}(P) = k_{nm}^0 \exp\{[-\Delta V_{\text{TS}_{mn}-n}(P - P_0) + 0.5\Delta\kappa_{\text{T,TS}_{mn}-n}(P - P_0)^2]/RT\} \quad [\text{Eq. S9}]$$

where k_{nm}^0 is the rate constant connecting the states n and m at 1 bar; $\Delta V_{TS_{mn}-n}$ is the change in partial molar volume between the corresponding transition state (TS_{mn}) and state n ; $\Delta\kappa_{T,TS_{mn}-n}$ is the change in isothermal compressibility between transition state TS_{mn} and state n ; R is the universal gas constant, and T is the temperature in Kelvin. The set of 8 global parameters varied in the fit thus includes: $\{k_{FI}^0; k_{IF}^0; k_{IU}^0; k_{UI}^0; \Delta V_{TS_{IF-F}}; \Delta V_{TS_{IF-I}}; \Delta V_{TS_{IU-U}}; \Delta V_{TS_{UI-I}}\}$ for model 1, plus 4 additional global parameters for model 2: $\{\Delta\kappa_{TS_{IF-F}}; \Delta\kappa_{TS_{IF-I}}; \Delta\kappa_{TS_{IU-U}}; \Delta\kappa_{TS_{UI-I}}\}$.

The population of each state, p_n , is related to the rate constants k_{nm} through the condition of macroscopic reversibility, $p_n k_{nm} = p_m k_{mn}$, which for a three-state system in Scheme [S1] leads to the following expressions for population of each state:

$$p_F = 1/[1 + (k_{FI}/k_{IF}) + (k_{FI}/k_{IF})(1 + k_{IU}/k_{UI})] \quad [\text{Eq. S10}]$$

$$p_I = 1/[1 + (k_{IF}/k_{FI}) + (k_{IU}/k_{UI})] \quad [\text{Eq. S11}]$$

and $p_U = 1 - p_F - p_I$. The uncertainties in the values of the optimized parameters, corresponding to confidence intervals of ± 1 standard deviation, were determined from the variance-covariance matrix of the non-linear fit. Convergence of the solution was confirmed by varying initial values for all parameters and obtaining the same solution within reported uncertainties.

Typical examples of the ^{15}N CPMG relaxation dispersion fits for FynSH3-VPL are shown in Figure S1. The values of the coefficients $\Delta\varpi_i^{m-n}$ (Eq. [S7]) obtained from the global fit for 46 residues in FynSH3-VPL are listed in Table S1, while the changes in chemical shifts, $\Delta\varpi_{F-I}$ and $\Delta\varpi_{F-U}$, calculated from the fitted $\Delta\varpi_i^{m-n}$ values for all pressures using the relationship in Eq. [S7], are listed in Table S2. The changes of both $\Delta\varpi_{F-I}$ and $\Delta\varpi_{F-U}$ with pressure are small. In fact, the absolute differences between $\Delta\varpi_{FI}$ and $\Delta\varpi_{FU}$ at the highest pressure used (2500 bar) and the corresponding values at 1 bar, $|\Delta\varpi_{m-n,2500} - \Delta\varpi_{m-n,1}|$ exceed 1 ppm for only 5 residues, with average values for $|\Delta\varpi_{F,I,2500} - \Delta\varpi_{F,I,1}|$ and $|\Delta\varpi_{F,U,2500} - \Delta\varpi_{F,U,1}|$ of 0.48 and 0.50 ppm, respectively. Figures S2A-B show the changes of $\Delta\varpi_{FI}$ and $\Delta\varpi_{FU}$ as a function of pressure for the residues with $|\Delta\varpi_{m-n,2500} - \Delta\varpi_{m-n,1}| \geq 1$ ppm. The values of $|\Delta\varpi_{m-n,2500} - \Delta\varpi_{m-n,1}|$ are shown as a function of residue number in Figures S2C-D. Somewhat larger values can be noticed for $\Delta\varpi_{FI}$ in the N- and C-termini of FynSH3-VPL (Figure 2C) where the structural differences between **F** and **I** are largest.

Figure S3 shows the dependence of intrinsic R_2 relaxation rates (s^{-1}) on pressure for the four residues of FynSH3-VPL which exhibit the largest differences between 2500 bar and 1 bar at 800 MHz (see Table S3 for the full list of the fitted R_2 rates). Note that because of the complex dependence of the viscosity of water on pressure, the R_2 rates were not constrained to any particular pressure-dependence during the fitting procedure. The average increase in R_2 between 1 and 2500 bar is $\sim 9\%$ at 800 MHz.

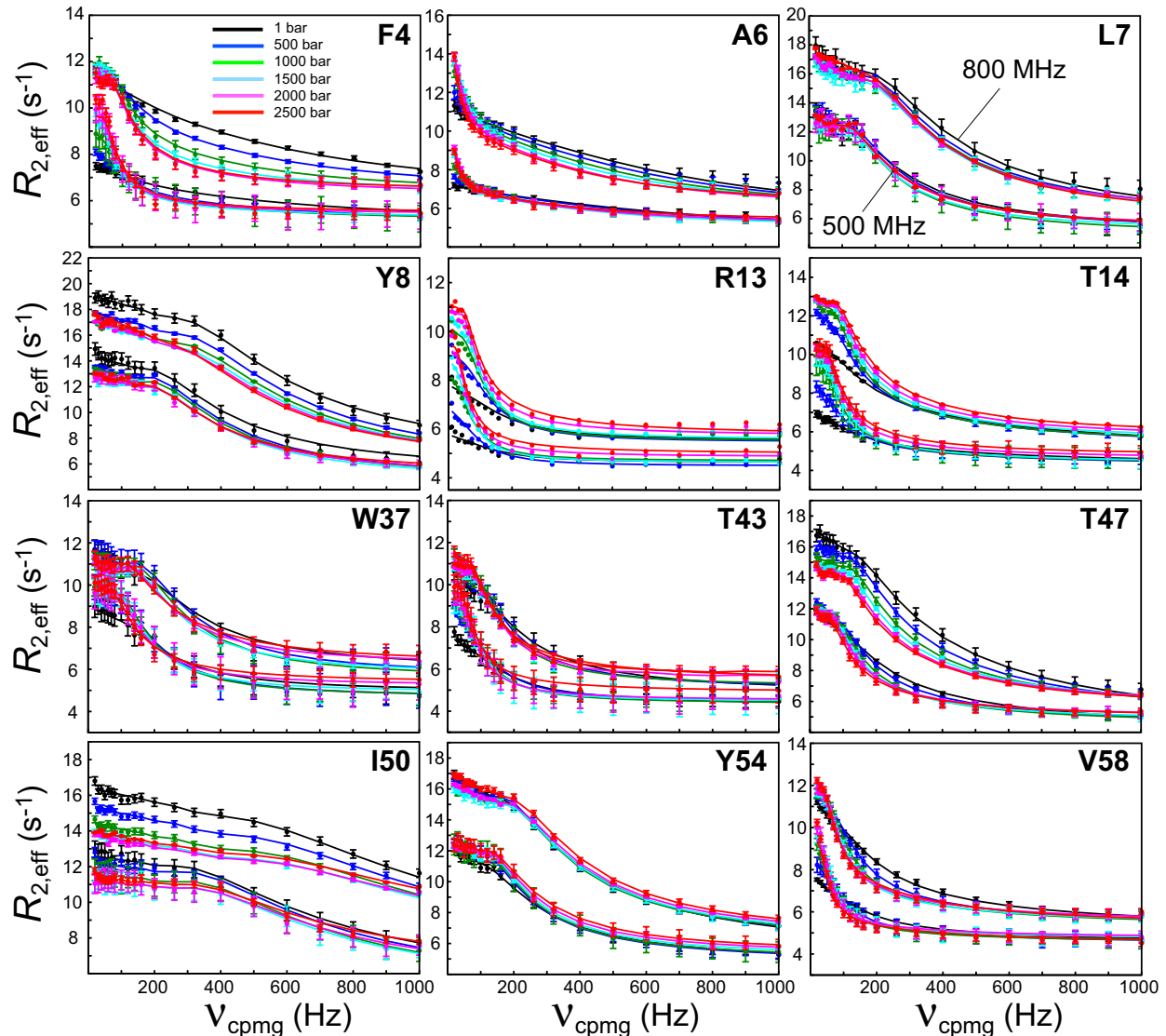


Figure S1. ^{15}N CPMG relaxation dispersion profiles recorded at six different pressures at 500 MHz and 800 MHz for selected residues of FynSH3-VPL. The color coding is the same as in Figures 1B and C of the main text.

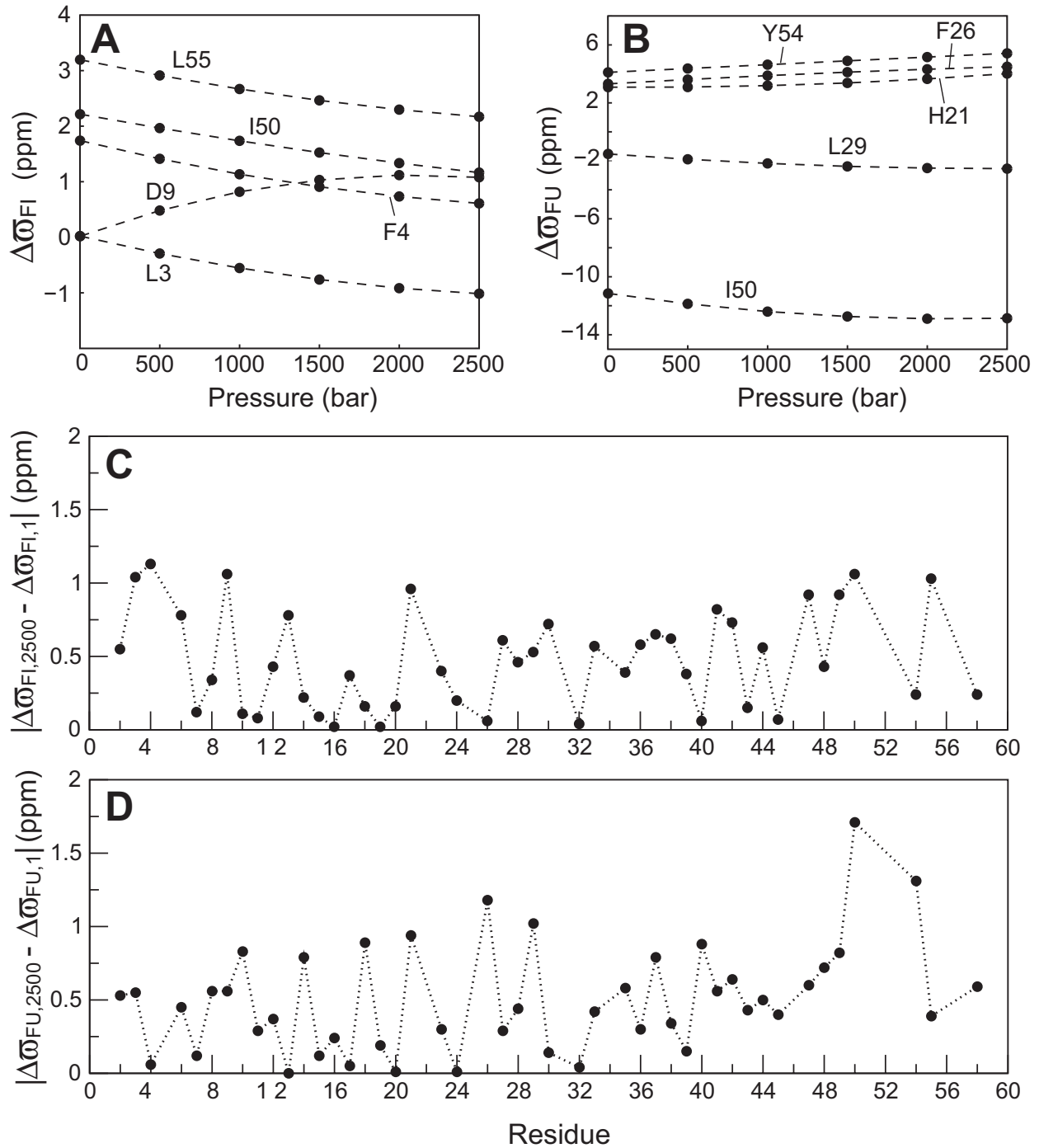


Figure S2. Changes in (A) $\Delta\omega_{FI}$ and (B) $\Delta\omega_{FU}$ (ppm) as a function of pressure for selected residues of FynSH3-VPL. See Table S2 for the full list of $\Delta\omega$'s as a function of pressure. Plots of absolute differences between (C) $\Delta\omega_{FI}$ and (D) $\Delta\omega_{FU}$ at the highest pressure used (2500 bar) and the corresponding values at 1 bar as a function of residue number.

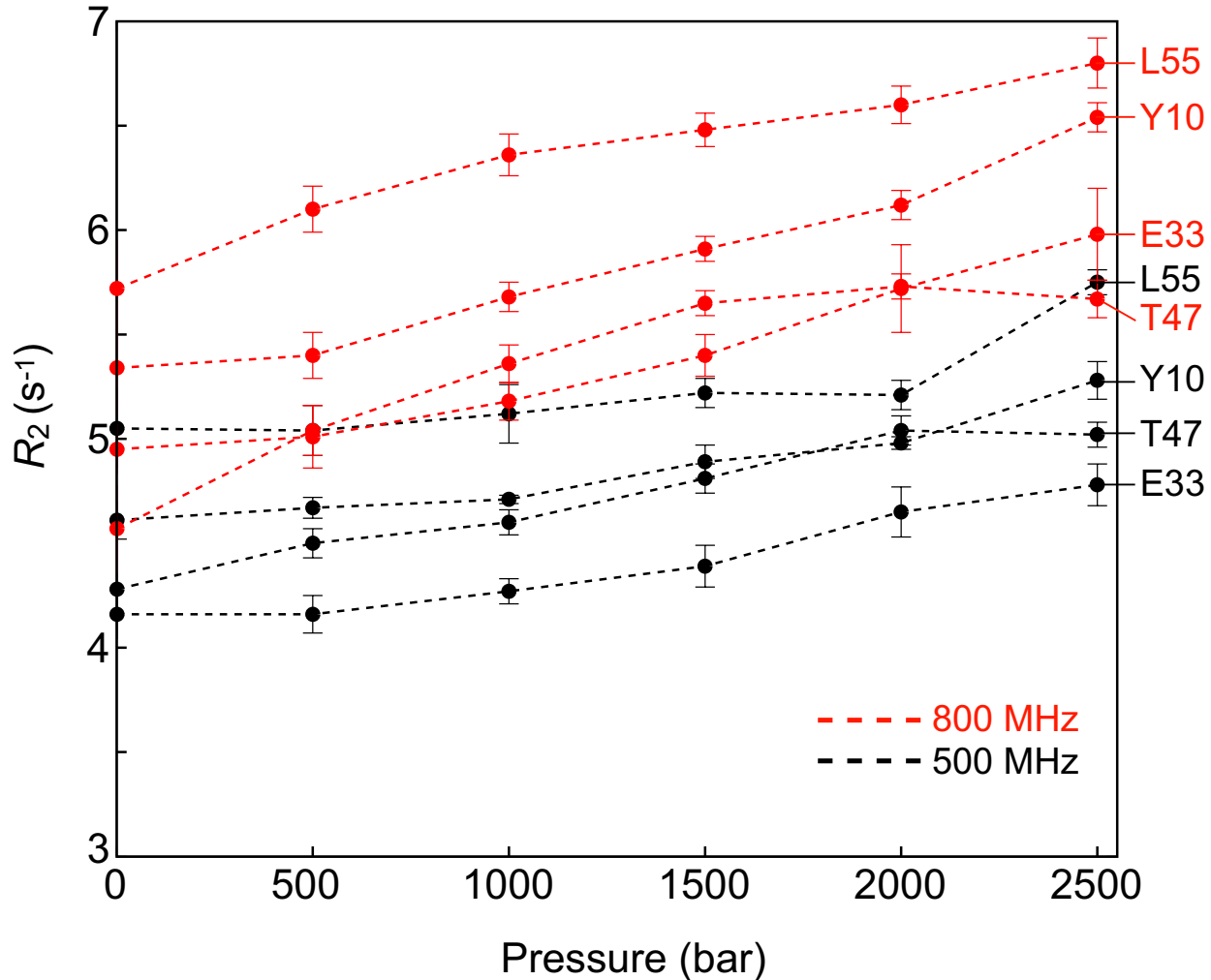


Figure S3. Dependence of R_2 relaxation rates (s^{-1}) on pressure for selected residues of FynSH3-VPL at 500 MHz (black circles and dashed lines) and 800 MHz (red circles and dashed lines). See Table S3 for the full list of R_2 rates at six different pressures.

Table S1. Values of the coefficients $\Delta\sigma_i^{m-n}$ obtained from the global fit for 46 residues of FynSH3-VPL.^{a)}

	$\Delta\sigma_0^{\text{F-I}}$ (ppm)	$\Delta\sigma_1^{\text{F-I}}$ $\times 10^3$ (ppm/bar)	$\Delta\sigma_2^{\text{F-I}}$ $\times 10^6$ (ppm/bar ²)	$\Delta\sigma_0^{\text{F-U}}$ (ppm)	$\Delta\sigma_1^{\text{F-U}}$ $\times 10^3$ (ppm/bar)	$\Delta\sigma_2^{\text{F-U}}$ $\times 10^6$ (ppm/bar ²)
T2	1.48 (0.29)	-0.28 (0.41)	0.02 (0.14)	1.22 (0.24)	-0.43 (0.30)	0.09 (0.09)
L3	0.02 (0.17)	-0.68 (0.25)	0.11 (0.08)	-1.61 (0.05)	0.75 (0.08)	-0.21 (0.03)
F4	1.74 (0.08)	-0.71 (0.17)	0.10 (0.06)	-1.72 (0.07)	0.42 (0.12)	-0.16 (0.04)
A6	2.30 (0.10)	-0.26 (0.13)	-0.02 (0.04)	-0.00 (0.07)	0.55 (0.09)	-0.15 (0.03)
L7	2.45 (0.11)	-0.29 (0.15)	0.09 (0.05)	4.80 (0.16)	-0.09 (0.33)	0.05 (0.11)
Y8	2.73 (0.12)	-0.19 (0.15)	0.02 (0.05)	7.65 (0.20)	0.80 (0.29)	-0.23 (0.10)
D9	0.02 (0.27)	1.05 (0.32)	-0.25 (0.10)	-4.62 (0.23)	0.45 (0.38)	-0.09 (0.15)
Y10	2.60 (0.12)	0.39 (0.16)	-0.17 (0.05)	-1.26 (0.09)	0.48 (0.13)	-0.06 (0.04)
E11	0.48 (0.46)	-1.09 (1.27)	0.42 (0.48)	6.83 (0.72)	-0.00 (1.05)	-0.04 (0.34)
A12	0.00 (0.33)	0.30 (0.50)	-0.19 (0.17)	-2.30 (0.14)	0.47 (0.20)	-0.13 (0.07)
R13	0.01 (0.43)	-0.33 (0.45)	0.01 (0.12)	-1.29 (0.11)	0.11 (0.14)	-0.04 (0.04)
T14	1.55 (0.06)	-0.18 (0.08)	0.03 (0.03)	1.22 (0.03)	0.42 (0.05)	-0.04 (0.02)
E15	0.38 (0.37)	-1.03 (1.08)	0.40 (0.42)	3.28 (0.33)	0.04 (0.52)	-0.04 (0.19)
D16	0.29 (0.24)	-0.98 (0.61)	0.39 (0.24)	4.11 (0.25)	-0.00 (0.36)	0.04 (0.13)
D17	0.00 (0.17)	0.52 (0.21)	-0.15 (0.07)	-0.66 (0.04)	-0.10 (0.05)	0.03 (0.01)
L18	0.51 (0.16)	-1.04 (0.32)	0.44 (0.11)	2.74 (0.11)	-0.39 (0.15)	0.01 (0.05)
S19	0.65 (0.07)	0.03 (0.13)	-0.01 (0.05)	0.59 (0.04)	-0.07 (0.06)	0.06 (0.02)
F20	0.00 (0.45)	0.62 (0.99)	-0.27 (0.37)	-4.55 (0.39)	-1.13 (0.54)	0.45 (0.18)
H21	0.47 (0.21)	-0.44 (0.36)	0.02 (0.12)	3.08 (0.20)	-0.07 (0.30)	0.18 (0.10)
G23	0.70 (0.22)	-1.03 (0.52)	0.35 (0.20)	5.90 (0.37)	-0.13 (0.57)	0.00 (0.20)
E24	1.13 (0.13)	-0.76 (0.17)	0.27 (0.05)	3.10 (0.18)	0.06 (0.24)	-0.03 (0.08)
F26	1.98 (0.11)	-0.22 (0.14)	0.08 (0.04)	3.31 (0.18)	0.63 (0.26)	-0.06 (0.09)
Q27	1.12 (0.09)	-0.67 (0.12)	0.17 (0.05)	2.04 (0.09)	0.08 (0.11)	-0.08 (0.04)
I28	1.54 (0.14)	-0.57 (0.20)	0.16 (0.06)	-2.56 (0.08)	-0.53 (0.12)	0.14 (0.04)
L29	1.42 (0.19)	-1.13 (0.32)	0.37 (0.11)	-1.52 (0.12)	-0.82 (0.18)	0.17 (0.06)
N30	0.00 (0.34)	-0.04 (0.68)	0.13 (0.24)	-3.98 (0.28)	-0.46 (0.45)	0.16 (0.15)
S32	0.21 (0.42)	-0.24 (0.60)	0.10 (0.25)	0.60 (0.14)	-0.00 (0.15)	0.01 (0.05)
E33	0.01 (2.61)	0.10 (2.86)	-0.13 (0.78)	-0.25 (0.37)	-0.01 (0.43)	-0.06 (0.12)
D35	0.00 (1.67)	-0.07 (2.00)	-0.03 (0.57)	-0.71 (0.40)	-0.52 (0.50)	0.12 (0.15)
W36	2.38 (0.09)	-0.23 (0.11)	0.00 (0.03)	1.26 (0.03)	-0.20 (0.04)	0.03 (0.01)
W37	0.00 (0.28)	-0.63 (0.43)	0.36 (0.14)	-3.57 (0.23)	-0.14 (0.33)	0.18 (0.11)
E38	0.41 (0.50)	0.15 (0.84)	-0.16 (0.29)	-2.32 (0.14)	-0.26 (0.25)	0.05 (0.09)
V39	0.00 (0.48)	-0.11 (0.72)	-0.02 (0.24)	-0.85 (0.10)	0.22 (0.15)	-0.06 (0.05)
R40	0.06 (0.48)	0.36 (1.45)	-0.15 (0.59)	-4.85 (0.44)	-1.02 (0.77)	0.27 (0.30)
S41	0.81 (0.58)	-0.35 (0.91)	0.01 (0.31)	-2.72 (0.19)	-0.51 (0.29)	0.11 (0.10)
L42	0.00 (0.39)	0.47 (0.55)	-0.07 (0.19)	-6.59 (0.42)	-0.68 (0.71)	0.17 (0.27)
T43	1.10 (0.16)	-0.57 (0.24)	0.21 (0.08)	2.04 (0.13)	-0.19 (0.21)	0.01 (0.07)
T44	0.07 (0.75)	-0.02 (1.18)	0.10 (0.39)	-6.07 (0.70)	-1.69 (0.95)	0.60 (0.29)
G45	0.37 (0.14)	0.05 (0.19)	-0.01 (0.06)	-0.51 (0.03)	0.32 (0.05)	-0.07 (0.02)
T47	2.70 (0.12)	-0.72 (0.15)	0.14 (0.05)	3.10 (0.10)	-0.12 (0.15)	-0.05 (0.05)
G48	1.82 (0.07)	-0.31 (0.09)	0.05 (0.03)	2.48 (0.06)	-0.40 (0.07)	0.05 (0.02)
Y49	0.44 (0.08)	0.98 (0.18)	-0.54 (0.06)	-0.62 (0.02)	-0.36 (0.05)	0.01 (0.02)
I50	2.22 (0.14)	-0.52 (0.16)	0.04 (0.05)	-11.15 (0.55)	-1.63 (0.81)	0.38 (0.26)
Y54	2.34 (0.10)	-0.28 (0.13)	0.07 (0.04)	4.11 (0.13)	0.53 (0.21)	-0.00 (0.08)
L55	3.20 (0.14)	-0.61 (0.17)	0.08 (0.05)	5.45 (0.18)	0.81 (0.30)	-0.26 (0.11)
V58	1.39 (0.09)	-0.40 (0.15)	0.12 (0.05)	1.58 (0.07)	-0.41 (0.10)	0.07 (0.03)

^{a)} Standard errors obtained from the variance-covariance matrix of the global fit are listed in parentheses.

Table S2. Values of $\Delta\varpi_{\text{F-I}}$ and $\Delta\varpi_{\text{F-U}}$ (ppm) obtained for 46 residues of FynSH3-VPL at six pressure values.^{a)}

	$\Delta\varpi_{\text{F-I}}(P)$							$\Delta\varpi_{\text{F-U}}(P)$						
	1	500	1000	1500	2000	2500	(bar)	1	500	1000	1500	2000	2500	(bar)
T2	1.48	1.35	1.22	1.11	1.01	0.93		1.22	1.03	0.88	0.77	0.71	0.69	
L3	0.02	-0.29	-0.55	-0.76	-0.92	-1.02		-1.61	-1.29	-1.07	-0.96	-0.96	-1.06	
F4	1.74	1.41	1.13	0.91	0.73	0.61		-1.72	-1.55	-1.46	-1.45	-1.51	-1.66	
A6	2.30	2.17	2.02	1.87	1.70	1.52		0.00	0.24	0.40	0.49	0.51	0.45	
L7	2.45	2.33	2.26	2.24	2.26	2.33		4.80	4.77	4.76	4.79	4.84	4.92	
Y8	2.73	2.64	2.56	2.50	2.44	2.39		7.65	7.99	8.22	8.33	8.33	8.21	
D9	0.02	0.48	0.82	1.03	1.12	1.08		-4.62	-4.42	-4.26	-4.15	-4.08	-4.06	
Y10	2.60	2.75	2.82	2.80	2.69	2.49		-1.26	-1.04	-0.84	-0.68	-0.54	-0.43	
E11	0.48	0.04	-0.18	-0.20	-0.00	0.40		6.83	6.81	6.78	6.72	6.64	6.54	
A12	0.00	0.10	0.11	0.03	-0.15	-0.43		-2.30	-2.10	-1.96	-1.89	-1.87	-1.93	
R13	0.01	-0.15	-0.31	-0.47	-0.62	-0.77		-1.29	-1.25	-1.23	-1.22	-1.25	-1.29	
T14	1.55	1.47	1.41	1.37	1.34	1.33		1.22	1.42	1.60	1.76	1.89	2.01	
E15	0.38	-0.04	-0.25	-0.27	-0.09	0.29		3.28	3.29	3.28	3.26	3.22	3.16	
D16	0.29	-0.11	-0.31	-0.31	-0.12	0.27		4.11	4.12	4.15	4.20	4.26	4.35	
D17	0.00	0.22	0.37	0.45	0.45	0.37		-0.66	-0.70	-0.72	-0.74	-0.73	-0.71	
L18	0.51	0.10	-0.09	-0.06	0.19	0.67		2.74	2.55	2.36	2.18	2.01	1.85	
S19	0.65	0.66	0.67	0.68	0.67	0.67		0.59	0.58	0.58	0.62	0.69	0.78	
F20	0.00	0.24	0.35	0.32	0.15	-0.16		-4.55	-5.00	-5.23	-5.23	-5.00	-4.54	
H21	0.47	0.25	0.05	-0.14	-0.32	-0.49		3.08	3.09	3.19	3.37	3.65	4.02	
G23	0.70	0.27	0.02	-0.06	0.03	0.30		5.90	5.84	5.78	5.71	5.66	5.60	
E24	1.13	0.82	0.65	0.60	0.70	0.93		3.10	3.12	3.14	3.13	3.12	3.09	
F26	1.98	1.89	1.84	1.83	1.85	1.92		3.31	3.61	3.88	4.12	4.32	4.49	
Q27	1.12	0.83	0.62	0.50	0.46	0.51		2.04	2.06	2.04	1.98	1.89	1.75	
I28	1.54	1.29	1.12	1.03	1.01	1.08		-2.56	-2.79	-2.95	-3.04	-3.06	-3.00	
L29	1.42	0.94	0.65	0.55	0.63	0.89		-1.52	-1.89	-2.18	-2.38	-2.50	-2.54	
N30	0.00	0.01	0.09	0.23	0.44	0.72		-3.98	-4.16	-4.27	-4.30	-4.25	-4.12	
S32	0.21	0.12	0.07	0.08	0.14	0.25		0.60	0.60	0.60	0.61	0.62	0.64	
E33	0.01	0.03	-0.02	-0.14	-0.32	-0.56		-0.25	-0.27	-0.32	-0.41	-0.52	-0.67	
D35	0.00	-0.04	-0.11	-0.18	-0.28	-0.39		-0.71	-0.95	-1.12	-1.23	-1.29	-1.29	
W36	2.38	2.26	2.14	2.03	1.91	1.80		1.26	1.17	1.09	1.03	0.99	0.96	
W37	0.00	-0.22	-0.27	-0.15	0.16	0.65		-3.57	-3.60	-3.53	-3.37	-3.12	-2.78	
E38	0.41	0.45	0.40	0.28	0.08	-0.21		-2.32	-2.44	-2.53	-2.60	-2.64	-2.66	
V39	0.00	-0.06	-0.12	-0.20	-0.29	-0.38		-0.85	-0.76	-0.70	-0.67	-0.67	-0.70	
R40	0.06	0.20	0.27	0.26	0.17	0.00		-4.85	-5.29	-5.60	-5.78	-5.82	-5.73	
S41	0.81	0.63	0.47	0.30	0.14	-0.01		-2.72	-2.94	-3.11	-3.22	-3.28	-3.28	
L42	0.00	0.22	0.40	0.54	0.66	0.73		-6.59	-6.89	-7.10	-7.23	-7.28	-7.23	
T43	1.10	0.86	0.73	0.70	0.77	0.95		2.04	1.94	1.85	1.77	1.69	1.61	
T44	0.07	0.09	0.15	0.26	0.42	0.63		-6.07	-6.76	-7.16	-7.26	-7.06	-6.57	
G45	0.37	0.39	0.41	0.43	0.44	0.44		-0.51	-0.36	-0.25	-0.17	-0.12	-0.11	
T47	2.70	2.37	2.12	1.94	1.82	1.78		3.10	3.03	2.93	2.81	2.67	2.50	
G48	1.82	1.68	1.57	1.48	1.42	1.39		2.48	2.29	2.13	1.98	1.86	1.76	
Y49	0.44	0.80	0.88	0.70	0.24	-0.48		-0.62	-0.80	-0.97	-1.13	-1.29	-1.44	
I50	2.22	1.97	1.74	1.53	1.33	1.16		-11.15	-11.87	-12.40	-12.74	-12.90	-12.86	
Y54	2.34	2.22	2.14	2.09	2.08	2.10		4.11	4.37	4.64	4.90	5.16	5.42	
L55	3.20	2.91	2.67	2.46	2.30	2.17		5.45	5.79	6.00	6.07	6.02	5.84	
V58	1.39	1.22	1.11	1.06	1.08	1.15		1.58	1.39	1.24	1.12	1.04	0.99	

^{a)} All the values are listed in ppm, and calculated using Eqs. [S7] and the coefficients $\Delta\varpi_i^{m-n}$ listed in Table S1.

Table S3. R_2 relaxation rates (s^{-1}) for 46 residues of FynSH3-VPL at 500 and 800 MHz fitted at six different pressures.^{a)}

	1 bar	500 bar	1000 bar	1500 bar	2000 bar	2500 bar						
	R_2^{500}	R_2^{800}										
T2	3.90 (0.17)	4.80 (0.43)	3.80 (0.17)	4.74 (0.23)	3.69 (0.17)	4.74 (0.25)	3.77 (0.13)	4.87 (0.21)	4.07 (0.14)	5.03 (0.19)	4.10 (0.13)	5.03 (0.23)
L3	4.45 (0.02)	5.66 (0.05)	4.49 (0.04)	5.63 (0.06)	4.60 (0.10)	5.71 (0.07)	4.62 (0.06)	5.84 (0.09)	4.83 (0.08)	5.87 (0.11)	4.91 (0.07)	6.03 (0.13)
F4	5.15 (0.05)	6.37 (0.10)	5.09 (0.04)	6.42 (0.06)	5.16 (0.13)	6.35 (0.09)	5.27 (0.04)	6.33 (0.09)	5.42 (0.13)	6.31 (0.09)	5.52 (0.06)	6.45 (0.12)
A6	4.89 (0.08)	5.56 (0.19)	5.00 (0.05)	5.74 (0.12)	5.02 (0.05)	5.85 (0.11)	5.05 (0.04)	5.97 (0.08)	5.20 (0.04)	6.03 (0.08)	5.37 (0.05)	6.20 (0.11)
L7	5.12 (0.16)	5.78 (0.22)	5.22 (0.10)	5.91 (0.07)	4.96 (0.18)	6.10 (0.11)	5.17 (0.10)	6.14 (0.14)	5.44 (0.15)	6.21 (0.08)	5.37 (0.02)	5.98 (0.04)
Y8	5.46 (0.16)	6.30 (0.20)	4.84 (0.05)	5.76 (0.08)	4.85 (0.06)	5.63 (0.04)	4.79 (0.05)	5.69 (0.04)	5.07 (0.08)	5.79 (0.04)	5.31 (0.05)	5.86 (0.09)
D9	4.70 (0.14)	5.90 (0.17)	4.64 (0.14)	5.63 (0.18)	4.47 (0.12)	5.29 (0.18)	4.46 (0.10)	5.05 (0.15)	4.60 (0.04)	5.15 (0.12)	4.95 (0.13)	5.53 (0.21)
Y10	4.61 (0.09)	5.34 (0.22)	4.67 (0.05)	5.40 (0.11)	4.71 (0.02)	5.68 (0.07)	4.89 (0.08)	5.91 (0.06)	4.98 (0.03)	6.12 (0.07)	5.28 (0.09)	6.54 (0.07)
E11	4.88 (0.43)	5.80 (0.54)	4.61 (0.21)	5.38 (0.18)	4.48 (0.17)	5.12 (0.16)	4.54 (0.12)	5.17 (0.22)	4.81 (0.14)	5.58 (0.09)	5.18 (0.10)	5.91 (0.18)
A12	4.49 (0.09)	5.12 (0.14)	4.43 (0.08)	5.05 (0.12)	4.50 (0.13)	5.04 (0.11)	4.61 (0.07)	5.23 (0.09)	4.80 (0.07)	5.49 (0.07)	4.99 (0.11)	5.68 (0.14)
R13	4.64 (0.04)	5.53 (0.11)	4.50 (0.03)	5.47 (0.10)	4.70 (0.09)	5.51 (0.10)	4.64 (0.09)	5.58 (0.09)	4.87 (0.02)	5.74 (0.06)	5.01 (0.04)	5.80 (0.09)
T14	4.38 (0.04)	5.21 (0.04)	4.31 (0.07)	5.29 (0.05)	4.37 (0.12)	5.38 (0.03)	4.42 (0.10)	5.58 (0.04)	4.65 (0.04)	5.73 (0.03)	4.82 (0.07)	5.90 (0.00)
E15	4.58 (0.22)	5.38 (0.30)	4.44 (0.26)	5.26 (0.23)	4.32 (0.19)	5.05 (0.25)	4.41 (0.13)	5.08 (0.27)	4.74 (0.17)	5.46 (0.16)	4.98 (0.17)	5.86 (0.24)
D16	4.18 (0.16)	4.97 (0.21)	4.13 (0.20)	4.85 (0.15)	4.05 (0.12)	4.67 (0.16)	4.12 (0.06)	4.76 (0.17)	4.33 (0.03)	5.13 (0.11)	4.67 (0.09)	5.50 (0.13)
D17	4.70 (0.03)	5.63 (0.02)	4.71 (0.04)	5.56 (0.05)	4.67 (0.03)	5.49 (0.05)	4.75 (0.02)	5.61 (0.05)	5.19 (0.06)	6.02 (0.06)	5.02 (0.04)	5.94 (0.09)
L18	4.13 (0.05)	4.89 (0.13)	4.15 (0.07)	5.06 (0.09)	4.29 (0.09)	4.99 (0.08)	4.53 (0.04)	5.19 (0.08)	4.02 (0.07)	5.23 (0.56)	4.89 (0.07)	5.46 (0.11)
S19	4.22 (0.03)	4.80 (0.05)	4.21 (0.02)	4.84 (0.03)	4.28 (0.04)	4.94 (0.04)	4.38 (0.03)	4.97 (0.05)	4.45 (0.04)	5.08 (0.06)	4.51 (0.05)	5.26 (0.10)
F20	5.33 (0.28)	6.52 (0.27)	5.00 (0.17)	5.91 (0.17)	4.75 (0.19)	5.70 (0.24)	4.91 (0.10)	5.79 (0.25)	5.30 (0.07)	6.30 (0.10)	5.69 (0.07)	6.73 (0.10)
H21	4.91 (0.20)	5.75 (0.22)	5.01 (0.07)	5.71 (0.11)	4.93 (0.03)	5.61 (0.09)	4.96 (0.17)	5.66 (0.08)	5.42 (0.08)	5.80 (0.10)	5.70 (0.08)	6.35 (0.15)
G23	5.39 (0.25)	6.03 (0.33)	5.14 (0.12)	5.76 (0.16)	5.05 (0.09)	5.54 (0.07)	5.00 (0.08)	5.61 (0.07)	5.38 (0.05)	5.86 (0.07)	5.56 (0.07)	6.27 (0.12)
E24	5.38 (0.18)	6.38 (0.24)	5.47 (0.11)	6.49 (0.12)	5.43 (0.11)	6.55 (0.08)	5.59 (0.10)	6.71 (0.07)	5.63 (0.09)	6.89 (0.05)	6.00 (0.06)	6.99 (0.07)
F26	4.72 (0.20)	5.31 (0.27)	4.78 (0.09)	5.53 (0.12)	4.94 (0.03)	5.63 (0.07)	5.15 (0.10)	5.75 (0.05)	5.24 (0.04)	5.95 (0.05)	5.51 (0.11)	6.01 (0.10)
Q27	5.06 (0.05)	5.87 (0.10)	5.12 (0.06)	5.93 (0.08)	5.08 (0.04)	5.96 (0.06)	5.20 (0.10)	6.03 (0.02)	5.41 (0.15)	6.12 (0.08)	5.75 (0.11)	6.34 (0.11)
I28	5.16 (0.07)	6.18 (0.22)	5.07 (0.13)	6.25 (0.13)	5.17 (0.03)	6.27 (0.11)	5.18 (0.10)	6.30 (0.11)	5.46 (0.11)	6.38 (0.08)	5.59 (0.05)	6.40 (0.11)
L29	5.10 (0.10)	5.92 (0.26)	5.25 (0.11)	6.23 (0.13)	5.25 (0.10)	6.29 (0.12)	5.36 (0.05)	6.40 (0.12)	5.41 (0.08)	6.45 (0.11)	5.82 (0.07)	6.40 (0.14)
N30	4.69 (0.20)	5.45 (0.22)	4.57 (0.11)	5.23 (0.14)	4.53 (0.15)	5.15 (0.11)	4.66 (0.14)	5.22 (0.14)	4.90 (0.11)	5.45 (0.18)	5.25 (0.10)	5.61 (0.17)
S32	4.10 (0.04)	4.80 (0.10)	4.11 (0.06)	4.82 (0.07)	4.20 (0.06)	4.86 (0.07)	4.26 (0.06)	4.98 (0.08)	4.45 (0.02)	5.21 (0.07)	4.60 (0.06)	5.46 (0.12)
E33	4.16 (0.12)	4.95 (0.12)	4.16 (0.09)	5.01 (0.15)	4.27 (0.06)	5.18 (0.09)	4.39 (0.10)	5.40 (0.10)	4.65 (0.12)	5.72 (0.21)	4.78 (0.10)	5.98 (0.22)
D35	4.71 (0.10)	5.10 (0.23)	4.18 (0.20)	5.07 (0.19)	4.24 (0.10)	4.93 (0.17)	4.29 (0.14)	4.92 (0.17)	4.41 (0.11)	5.06 (0.17)	4.49 (0.14)	5.33 (0.23)
W36	4.42 (0.05)	5.46 (0.09)	4.45 (0.04)	5.56 (0.05)	4.46 (0.02)	5.72 (0.03)	4.55 (0.04)	5.90 (0.04)	4.84 (0.02)	6.10 (0.02)	5.00 (0.04)	6.25 (0.04)
W37	4.97 (0.19)	6.03 (0.18)	4.71 (0.16)	5.72 (0.16)	4.73 (0.11)	5.59 (0.12)	4.93 (0.14)	5.78 (0.07)	5.26 (0.17)	6.23 (0.06)	5.40 (0.11)	6.30 (0.21)
E38	5.06 (0.17)	5.84 (0.30)	4.98 (0.10)	5.60 (0.20)	4.96 (0.13)	5.53 (0.15)	5.00 (0.10)	5.77 (0.14)	5.27 (0.07)	6.09 (0.07)	5.58 (0.11)	6.43 (0.14)
V39	5.34 (0.05)	6.47 (0.06)	5.43 (0.02)	6.41 (0.05)	5.49 (0.04)	6.47 (0.05)	5.49 (0.11)	6.57 (0.07)	5.75 (0.05)	6.70 (0.10)	5.76 (0.08)	6.87 (0.10)
R40	5.27 (0.31)	6.12 (0.26)	5.02 (0.18)	5.71 (0.16)	4.98 (0.15)	5.52 (0.26)	5.00 (0.13)	5.63 (0.30)	5.20 (0.09)	6.03 (0.19)	5.80 (0.11)	6.58 (0.08)
S41	5.33 (0.22)	6.01 (0.51)	5.04 (0.15)	5.79 (0.26)	5.09 (0.08)	5.75 (0.20)	5.16 (0.08)	6.03 (0.15)	5.43 (0.07)	6.36 (0.07)	5.87 (0.07)	6.88 (0.05)
L42	5.25 (0.20)	6.35 (0.21)	5.05 (0.12)	5.97 (0.16)	4.84 (0.17)	5.74 (0.18)	4.94 (0.14)	5.79 (0.23)	5.18 (0.13)	6.02 (0.22)	5.54 (0.18)	6.42 (0.29)
T43	4.29 (0.09)	4.89 (0.21)	4.44 (0.05)	5.06 (0.13)	4.38 (0.10)	5.18 (0.13)	4.48 (0.17)	5.25 (0.10)	4.53 (0.13)	5.49 (0.10)	4.93 (0.14)	5.53 (0.12)
T44	5.22 (0.39)	6.02 (0.32)	4.95 (0.14)	5.49 (0.16)	4.78 (0.09)	5.28 (0.14)	4.74 (0.17)	5.36 (0.22)	5.03 (0.27)	5.62 (0.27)	5.45 (0.09)	5.87 (0.20)
G45	4.81 (0.05)	5.44 (0.07)	4.74 (0.03)	5.39 (0.04)	4.82 (0.03)	5.52 (0.03)	4.88 (0.02)	5.58 (0.03)	4.98 (0.03)	5.69 (0.02)	5.12 (0.06)	5.86 (0.05)
T47	4.28 (0.08)	4.57 (0.21)	4.50 (0.07)	5.04 (0.12)	4.60 (0.06)	5.36 (0.09)	4.81 (0.07)	5.65 (0.06)	5.04 (0.07)	5.73 (0.06)	5.02 (0.06)	5.67 (0.09)
G48	5.00 (0.04)	5.57 (0.09)	5.02 (0.04)	5.77 (0.07)	5.07 (0.05)	5.94 (0.06)	5.28 (0.03)	6.04 (0.04)	5.38 (0.04)	6.15 (0.02)	5.57 (0.10)	6.21 (0.03)
Y49	4.82 (0.07)	6.00 (0.04)	4.88 (0.06)	5.89 (0.03)	4.99 (0.06)	5.68 (0.07)	4.89 (0.06)	5.86 (0.07)	5.10 (0.07)	6.33 (0.05)	5.33 (0.06)	6.49 (0.09)
I50	5.46 (0.24)	6.57 (0.34)	5.24 (0.12)	6.28 (0.17)	5.09 (0.15)	6.15 (0.11)	5.18 (0.14)	6.34 (0.09)	5.65 (0.13)	6.85 (0.07)	6.28 (0.05)	7.65 (0.03)
Y54	4.79 (0.11)	5.52 (0.17)	4.85 (0.08)	5.85 (0.09)	4.98 (0.16)	6.03 (0.05)	5.17 (0.03)	6.21 (0.08)	5.33 (0.04)	6.35 (0.05)	5.46 (0.11)	6.46 (0.10)
L55	5.05 (0.19)	5.72 (0.23)	5.04 (0.12)	6.10 (0.11)	5.12 (0.14)	6.36 (0.10)	5.22 (0.07)	6.48 (0.08)	5.21 (0.07)	6.60 (0.09)	5.75 (0.06)	6.80 (0.12)
V58	4.55 (0.04)	5.30 (0.11)	4.53 (0.08)	5.34 (0.08)	4.58 (0.07)	5.39 (0.09)	4.75 (0.08)	5.48 (0.10)	4.80 (0.07)	5.57 (0.08)	4.61 (0.04)	5.45 (0.07)

^{a)}All the rates are listed in s^{-1} . Standard errors obtained from the variance-covariance matrix of the global fit are indicated in parentheses.

Supplementary references

- 1 Neudecker, P. *et al.* Identification of a collapsed intermediate with non-native long-range interactions on the folding pathway of a pair of Fyn SH3 domain mutants by NMR relaxation dispersion spectroscopy. *J. Mol. Biol.* **363**, 958-976 (2006).
- 2 Neudecker, P. *et al.* Structure of an intermediate state in protein folding and aggregation. *Science* **336**, 362-366 (2012).
- 3 Kapust, R. B. *et al.* Tobacco etch virus protease: mechanism of autolysis and rational design of stable mutants with wild-type catalytic proficiency. *Protein Eng.* **14**, 993-1000 (2001).
- 4 Maxwell, K. L. & Davidson, A. R. Mutagenesis of a buried polar interaction in an SH3 domain: sequence conservation provides the best prediction of stability effects. *Biochemistry* **37**, 16172-16182 (1998).
- 5 Meiboom, S. & Gill, D. Modified spin-echo method for measuring nuclear relaxation times. *Rev. Sci. Instrum.* **29**, 688-691 (1958).
- 6 Hansen, D. F., Vallurupalli, P. & Kay, L. E. An improved ^{15}N relaxation dispersion experiment for the measurement of millisecond time-scale dynamics in proteins. *J. Phys. Chem. B* **112**, 5898-5904 (2008).
- 7 Millet, O., Loria, J.P., Kroenke, C.D., Pons, M. & Palmer, A.G. The static magnetic field dependence of chemical exchange line-broadening defines the NMR chemical shift time scale. *J. Am. Chem. Soc.* **122**, 2867-2877 (2001).